agreement with the 7.5-hr value originally reported by the discoverers of the element.[15] Our half-life for Bi^{207} agrees well with the lower limit set by Neumann and Perlman,[2] but is significantly greater than the values reported by Harbottle[5] and by Sosniak and Bell.[4] The reason for this discrepancy is not immediately apparent. The 8-year half-life obtained by Cheng *et al.*[3] is completely out of line, and it is difficult to believe that it pertains to the same isotope.

[15] D. Corson, K. MacKenzie, and E. Segrè, Phys. Rev. **57**, 459 (1940).

ACKNOWLEDGMENTS

The cyclotron bombardments were executed by the crew of the University of California's 60-in. cyclotron under Mr. W. B. Jones. I am grateful for the assistance of the Lawrence Radiation Laboratory's Health Chemistry Group in handling the targets. The americium used was purified by Mr. Denis McWhan, and the alpha counters were standardized by Mrs. Elinor Potter. The calculations on the IBM 704 were carried out under the direction of Miss Margaret Butler of the Argonne National Laboratory Applied Mathematics Division. I wish to thank Professor I. Perlman and Dr. Frank Asaro for much invaluable discussion.

PHYSICAL REVIEW VOLUME 121, NUMBER 1 JANUARY 1, 1961

Properties of Finite Nuclei

K. A. BRUECKNER*
University of California, La Jolla, California

A. M. LOCKETT
Los Alamos Scientific Laboratory, University of California, Los Alamos, New Mexico

AND

M. ROTENBERG
University of Chicago, Chicago, Illinois

(Received August 26, 1960)

The properties of O^{16}, Ca^{40}, and Zr^{90} have been determined, using the Brueckner-Gammel-Weitzner theory of finite nuclei. Self-consistent solutions of the Hartree-Fock equations as modified by Brueckner and Goldman have been obtained. The properties computed include binding energy, mean proton and neutron radii, separation energies, spin-orbit splittings, nonlocal and state-dependent single-particle potentials, surface depth of density and potentials, potential-density relation. The predictions of the theory are in semiquantitative agreement with experiment.

I. INTRODUCTION

IN a series of previous papers,[1] methods have been developed for the study of many-fermion systems and applied in detail to the determination of the properties of nuclear matter. Approximate extensions of these methods to the study of finite nuclei have also been proposed[2] It is the purpose of this paper to review briefly the formulation and present status of the methods as applied to nuclear matter, to describe the theory of finite nuclei, and to give the results of a numerical study of the properties of finite nuclei.

II. NUCLEAR MATTER

In this section we shall not attempt to review the basis of the procedures used in the study of nuclear matter, but give only a brief summary of the present status of the methods.

The results of this paper are based on the K-matrix approximation[1] for the ground-state energy of nuclear matter, which is

$$E=\sum_i \frac{p_i^2}{2m}+\tfrac{1}{2}\sum_{ij}(K_{ij,ij}-K_{ij,ji}). \tag{2.1}$$

The K matrix determines the interaction of pairs of nucleons moving in the nuclear medium, taking account of the exclusion principle and the binding effects of the average nuclear field. The determining equation for K is

$$K=v+vGK, \tag{2.2}$$

in which the propagator G describes motion in the nuclear field. Taking matrix elements of Eq. (2.2) with respect to the eigenstates of the unperturbed medium, we rewrite Eq. (2.2) as

$$K_{kl,ij}=v_{kl,ij}+\sum_{mn} v_{kl,mn}G_{mn}(ij)K_{mn,ij}, \tag{2.3}$$

* Supported in part by a grant from the Atomic Energy Commission.

[1] See K. A. Brueckner and J. L. Gammel, Phys. Rev. **109**, 1023 (1958), for a list of references.

[2] K. A. Brueckner, J. L. Gammel, and H. Weitzner, Phys. Rev. **110**, 431 (1958); R. J. Eden and V. J. Emery, Proc. Roy. Soc. (London) **A248**, 266 (1958); and R. J. Eden, V. J. Emery, and S. Sampanthar, Proc. Roy. Soc. (London) **A253**, 177 (1959).

with the propagator given by

$$G_{mn}(ij)=(E_i^*+E_j^*-E_m^*-E_n^*)^{1};\ p_m, p_n\geqq p_F$$
$$=0, \text{ otherwise.} \quad (2.4)$$

The energies of virtual particle and hole excitations in Eq. (2.4) are determined by the equations of the form

$$E_i^*=\frac{p_i^2}{2m}+\sum_j (K_{ij,ij}-K_{ij,ji}). \quad (2.5)$$

The energy as determined by these coupled equations is a function of both the set of basis functions chosen and the manner in which the states are filled. The former problem is relatively simple in nuclear matter since the eigenstates are plane waves and hence need not be solved by a separate procedure such as will be required in the finite nucleus. The problem of choosing the optimum unperturbed state or equivalently the manner of filling the states is, however, nontrivial. The original assumption of Brueckner[3] and of Goldstone,[4] that the best choice was the fully degenerate Fermi gas, can lead only to the lowest "normal state" of the nuclear matter. The presence of attractive forces at the Fermi surface leads to an alteration of level structure and a slight increase of the mean binding energy.[5] These effects may be very important in certain nuclear properties such as the low-lying collective nuclear states, but have a negligible effect on the total energy. Thus in determining average nuclear properties, these effects can be neglected. This approximation has been adopted in the results of this paper.

Other sources of error in the K-matrix approximation of Eq. (2.1) result from higher order corrections in the linked cluster expansion[3] for the total energy. The "ring diagrams," which are essential in some of the other applications of many-body theory,[6] perturb the nuclear system only very weakly. Numerical estimates of the leading cluster corrections show that the mean energy is shifted by a fraction of an Mev per particle. Other more important corrections arise from improvements in Eq. (2.5) for the single-particle energies. The effects of "off-energy-shell" propagation[1] change Eq. (2.4) when the energies of virtual excitations are determined. This effect has been introduced into Eq. (3.3) and Eq. (2.1) only approximately so that a residual error of a few tenths Mev probably remains in the ground-state energy per particle. Another correction to Eq. (2.5) arises from rearrangement effects in the single-particle energy.[7] Explicit calculations of these effects show that the ground-state energy is shifted by the order of an Mev.[8] The rearrangement corrections to the single-particle energies are much larger and cannot be neglected. It has been shown by Brueckner and Goldman,[9] however, that these corrections can be included in the treatment of finite nuclei so that the first-order error is eliminated.

To summarize: The K-matrix approximation of Eq. (2.1) for the total energy gives a result for the mean energy per particle with an error of about one Mev. If the same order of approximation could be maintained in finite nuclei, a similar error might be expected. We shall see, however, that certain additional approximations introduce further errors into the actual calculations for finite nuclei.

III. METHOD FOR FINITE NUCLEI

The detailed discussion of the theory of finite nuclei has been previously given.[2] We only summarize the theory here. We consider Eq. (2.2) for the K matrix. The form of Eq. (2.2) does not depend on the representation except through the implicit dependence of the propagator G on the energies of the single-particle states. To obtain a self-consistent solution in the sense of the nuclear matter calculations, in which the coupled equations [Eq. (2.3), Eq. (2.4), Eq. (2.5)] were solved by iteration, it is therefore necessary to redetermine the single-particle energies appropriate to the eigenstates of the finite system. These in turn can be determined only by a method similar to the self-consistent Hartree-Fock procedure. Consequently, a double self-consistency problem arises. To avoid this extremely difficult and probably at present insoluble problem, the approximation described previously has been adopted in this paper. This is based on the relative insensitivity of the propagator G of Eq. (2.4) to the representation. The energy differences entering into Eq. (2.4) are typically of the order of 50 to 100 Mev and not appreciably different in the finite system or nuclear matter. Thus the K-matrix dependence on G can be expressed only through the dependence of K on the local density of the finite nucleus, the self-consistent propagator G as determined in nuclear matter at the local density being used to evaluate K. This approximation would introduce a vanishing error if the correlation range in the K matrix were small compared to the distance over which the density changes appreciably. The correlation range is somewhat less than 10^{-13} cm, while the nuclear density drops at the nuclear surface from 90% to 10% of the central value in about 2.4×10^{-13} cm. Thus the correlation range is considerably less than the nuclear surface depth, and our basic approximation cannot be qualitatively in error, at least in determining mean properties. The error is probably more important in the

[3] K. A. Brueckner, Phys. Rev. **100**, 36 (1955).
[4] Goldstone, Proc. Roy. Soc. (London) **A235**, 408 (1956).
[5] A. Bohr, B. R. Mottelson, and D. Pines, Phys. Rev. **110**, 936 (1958).
[6] Murray Gell-Mann and Keith A. Brueckner, Phys. Rev. **106**, 364 (1957); K. Sawada, Phys. Rev. **106**, 372 (1957); K. A. Brueckner and K. Sawada, Phys. Rev. **106**, 1117 (1957).
[7] K. A. Brueckner, Phys. Rev. **110**, 597 (1958); N. M. Hugenholtz and L. van Hove, Physica **24**, 363 (1958).
[8] K. A. Brueckner, J. L. Gammel, and J. T. Kubis, Phys. Rev. **118**, 1438 (1960).
[9] K. A. Brueckner and D. T. Goldman, Phys. Rev. **117**, 207 (1960).

surface properties and surface energy; we shall return to this point in the discussion of our results.

Without giving more details of the K-matrix evaluation for the finite nucleus problem (we refer to the original papers for further discussion), we assume that the coordinate space operator

$$(r_1r_2|K(\rho)|r_1'r_2'), \tag{3.1}$$

is given. This has been derived, starting from the Gammel-Thaler two-body potentials with parameters given in Table I. The numerical values of K are tabulated in reference 2. Our problem is to determine a set of single-particle energy functions so that Eq. (2.1) gives the lowest energy for the finite nucleus. We start from a set $\varphi_i(r_i)$ and the product function for the N nucleons of the nucleus,

$$\Psi(1,\cdots,N)=A\,\varphi_1(r_1)\cdots\varphi_N(r_N). \tag{3.2}$$

The operator A is the usual antisymmetrizing operator,

$$A=\sum_p(-1)^p, \tag{3.3}$$

with the sum carried out over all pair permutations of the identical nucleons. The appropriate modification of Eq. (2.1) then is

$$E=\int\Psi^*(1,\cdots,N)\sum_{i=1}^{N}\frac{p_i^2}{2m}\Psi(1,\cdots,N)d\mathbf{r}_1\cdots d\mathbf{r}_N$$
$$+\frac{1}{2}\int\Psi(1,\cdots,N)\sum_{ij}(r_ir_j|K(\rho)|r_i'r_j')$$
$$\times\Psi(1',\cdots,N')d\mathbf{r}_1\cdots d\mathbf{r}_Nd\mathbf{r}_1'\cdots d\mathbf{r}_N'. \tag{3.4}$$

This is the basic equation which we use to determine the optimum form of the single-particle energy functions φ_i. To do this, we ask that E be stationary with respect to variations of the form of $\varphi_i^*(r)$, i.e.,

$$\delta E/\delta\varphi_i^*(r)=0\quad\text{(for all }i\text{)}. \tag{3.5}$$

To carry out this variation, we first simplify Eq. (3.4) to the form

$$E=\sum_i\int\varphi_i^*(r)\frac{p^2}{2m}\varphi_i(r)d\mathbf{r}+\tfrac{1}{2}\sum_{ij}\int\varphi_i^*(r_1)\varphi_j^*(r_2)$$
$$\times(r_1r_2|K(\rho)|r_1'r_2')(1-P_\sigma P_\tau)\varphi_i(r_1')\varphi_j(r_2')$$
$$\times d\mathbf{r}_1'd\mathbf{r}_2'd\mathbf{r}_1d\mathbf{r}_2, \tag{3.6}$$

with P_σ and P_τ the spin and isotopic spin exchange operators. The variation with respect to $\varphi_i^*(r)$ then gives the result

$$E_i\varphi_i(r)=\frac{p^2}{2m}\varphi_i(r)$$
$$+\int V_{\mathrm{HF}}(\mathbf{r},\mathbf{r}')\varphi_i(r')d\mathbf{r}'+V_R(r)\varphi_i(r), \tag{3.7}$$

TABLE I. Parameters of the Gammel-Thaler potentials. The potentials all have the Yukawa form outside of a repulsive core of radius 0.4×10^{-13} cm.

State	Strength (Mev)	Inverse range (10^{+13} cm^{-1})
Triplet central even	−877.39	2.0908
Tensor even	−159.40	1.0494
Spin-orbit even	−5000	3.70
Singlet even	−434.0	1.45
Triplet central odd	−14.0	1.00
Tensor odd	22.0	0.80
Spin-orbit odd	−7315	3.70
Singlet odd	130.0	1.00

with the two interaction terms V_{HF} and V_R the Hartree-Fock and rearrangement potentials. The former is given by the expression

$$V_{\mathrm{HF}}(r,r')=\sum_j\int d\mathbf{r}_1d\mathbf{r}_1'\;\varphi_j^*(r_1)(rr_1|K(\rho)|r'r_1')$$
$$\times(1-P_\sigma P_\tau)\varphi_j(r_1') \tag{3.8}$$

which is a generalization of the usual Hartree-Fock potential.

The rearrangement potential V_R results from the dependence of the K matrix on the density. The density is related to the single-particle functions:

$$\rho(R)=\sum_i\varphi_i^*(R)\varphi_i(R), \tag{3.9}$$

so that

$$\delta\rho(R)/\delta\varphi_i^*(r)=\varphi_i(r)\delta(\mathbf{r}-\mathbf{R}). \tag{3.10}$$

The density as it appears in the K matrix is evaluated at the center-of-gravity point, so that R in Eq. (3.10) is

$$R=\tfrac{1}{2}(\mathbf{r}_1+\mathbf{r}_2). \tag{3.11}$$

We further have used the approximation that the range of interaction in the density-dependent part of the K matrix is sufficiently short so that we can set $\mathbf{r}_1=\mathbf{r}_2$ in Eq. (3.11). In this approximation the variation of E with respect to $\varphi_i(r)$ gives the rearrangement term,

$$V_R(r)=\int d\mathbf{r}_2d\mathbf{r}_1'd\mathbf{r}_2'\;\varphi_i^*(r)\varphi_j^*(r_2)\frac{\partial}{\partial\rho}(r_1r_2|K(\rho)|r_1'r_2')$$
$$\times(1-P_\sigma P_\tau)\varphi_i(r_1')\varphi_j(r_2'). \tag{3.12}$$

The evaluation of Eq. (3.12) has been given by Brueckner and Goldman,[9] who show that a good approximation to $V_R(r)$ is

$$V_R(r)=240[\rho(r)]^2\ \mathrm{Mev}(10^{-13}\ \mathrm{cm})^6. \tag{3.13}$$

We shall describe the effect of this term in discussing our results.

The single-particle functions are finally determined from Eq. (3.7) and Eq. (3.8). The method of solving these coupled equations is described in the following sections.

IV. SOLUTION OF THE MODIFIED HARTREE-FOCK EQUATIONS

The details of the angular momentum reduction of Eq. (3.7) have been given by Brueckner, Gammel, and Weitzner[2] (we refer to this paper as BGW). We summarize the relevant formulas and refer to this paper for further discussion.

To determine the Hartree-Fock term in the potential of Eq. (3.7), an expression of the form [see Eq. (77) of BGW]

$$(\mathbf{r}_1|V|\mathbf{r}_1')=\sum_j\int d\mathbf{r}_2 d\mathbf{r}_2'\,\varphi_j^*(r_2)(\mathbf{r}_{12}|K|\mathbf{r}_{12}')\varphi_j(r_2'), \quad (4.1)$$

must be evaluated. To do so, we first separate the angular dependence of the wave function; writing

$$\varphi_j(\mathbf{r}_2)=\frac{R_{nlJ}(r_2)}{r_2}F_{Jls}^m(\mathbf{r}_2), \quad (4.2)$$

where $F_{Jls}^m(\mathbf{r}_2)$ is an eigenfunction of the total angular momentum. The sum over azimuthal quantum numbers then gives for a filled shell

$$\sum_m F_{Jls}^m(\mathbf{r}_2)^*F_{Jls}^m(\mathbf{r}_2')=\left(\frac{2l+1}{4\pi}\right)^{\frac{1}{2}}Y_1^0(\mathbf{r}_2,\mathbf{r}_2'). \quad (4.3)$$

The remaining sum over n, l, J is used to introduce new functions, i.e.,

$$H(\mathbf{r}_2,\mathbf{r}_2')=\sum_{nJl}\left(\frac{2l+1}{4\pi}\right)^{\frac{1}{2}}Y_1^0(\mathbf{r}_2,\mathbf{r}_2')\times\frac{R_{nJl}(r_2)}{r_2}\frac{R_{nJl}(r_2')}{r_2'}, \quad (4.4)$$

so that Eq. (4.1) becomes

$$(\mathbf{r}_1|V|\mathbf{r}_1')=\int d\mathbf{r}_2 d\mathbf{r}_2'(\mathbf{r}_{12}|K|\mathbf{r}_{12}')H(\mathbf{r}_2,\mathbf{r}_2'). \quad (4.5)$$

To evaluate Eq. (4.5), we first make use of the delta function in the K-matrix representing conservation of the center of mass, so that the integration over $\mathbf{r}_2'$ can be carried out and the replacement

$$\mathbf{r}_2'=\mathbf{r}_1+\mathbf{r}_2-\mathbf{r}_1', \quad (4.6)$$

made. We then change variable from $\mathbf{r}_2$ to $\mathbf{r}_{12}$ and define

$$\mathbf{x}=\mathbf{r}_1'-\mathbf{r}_1. \quad (4.7)$$

Equation (4.5) then becomes

$$(\mathbf{r}|V|\mathbf{r}_1+\mathbf{x})=\int d\mathbf{r}_{12}(\mathbf{r}_{12}|K|\mathbf{r}_{12}+2\mathbf{x})\times H(\mathbf{r}_1-\mathbf{r}_{12},\,\mathbf{r}_1-\mathbf{r}_{12}-\mathbf{x}). \quad (4.8)$$

To evaluate Eq. (4.8), the space and time limitation set by the computing capacity of the IBM 704 require certain simplification. This was done by retaining only the first two terms in the dependence of $(\mathbf{r}_1|V|\mathbf{r}_1+\mathbf{x})$ on the angle between $\mathbf{r}_1$ and $\mathbf{x}$, i.e., by assuming that the dependence can be represented approximately as

$$(\mathbf{r}_1|V|\mathbf{r}_1+\mathbf{x})=V_0(r_1,x)+V_1(r_1,x)\frac{\mathbf{x}\cdot\mathbf{r}_1}{xr_1}. \quad (4.9)$$

This approximation is based on the short range of the nonlocality in the nonlocal potential $(\mathbf{r}_1|V|\mathbf{r}_1')$. The term V_0 represents the spherically symmetric part and V_1 the part resulting from the variation of the nuclear density over the nonlocal range.

To determine V_0 and V_1 in Eq. (4.9), it is sufficient to evaluate $(\mathbf{r}_1|V|\mathbf{r}_1+\mathbf{x})$ for $\mathbf{x}$ parallel and antiparallel to $\mathbf{r}_1$. Calling these two values

$$\begin{aligned}V_+(r_1,x)&=(\mathbf{r}_1|V|\mathbf{r}_1+x\hat{r}_1),\\ V_-(r_1,x)&=(\mathbf{r}_1|V|\mathbf{r}_1-x\hat{r}_1),\end{aligned} \quad (4.10)$$

we find

$$\begin{aligned}V_0(r_1,x)&=\tfrac{1}{2}[V_+(r_1,x)+V_-(r_1,x)],\\ V_1(r_1,x)&=\tfrac{1}{2}[V_+(r_1,x)-V_-(r_1,x)].\end{aligned} \quad (4.11)$$

For this restricted choice of the relative direction of $\mathbf{x}$ and $\mathbf{r}_1$, we can also replace $\mathbf{r}_1$ in Eq. (4.8) by $\pm\mathbf{x}r_1/x$ with the sign determined by the choice of parallel or antiparallel orientation.

We now return to Eq. (4.8). We choose $\mathbf{x}$ as the polar axis and can immediately carry out the integration over the azimuthal angle of $\mathbf{r}_{12}$ since for our choice of the direction of $\mathbf{x}$, the integral is independent of the azimuthal angle. We then introduce a new variable by the transformation

$$|\mathbf{r}_{12}+2\mathbf{x}|=r_{12}+s, \quad (4.12)$$

or

$$\cos\theta=\frac{s^2+2r_{12}s-4x^2}{4xr_{12}}, \quad (4.13)$$

with θ the angle between $\mathbf{r}_{12}$ and $\mathbf{x}$. We also introduce the angular momentum decomposition of the K matrix, which is

$$(\mathbf{r}_{12}|K|\mathbf{r}_{12}+2\mathbf{x})=\sum_l(2l+1)(r_{12}|K_l|r_{12}+s)\times P_l\left(1-\frac{4x^2-s^2}{2r_{12}(r_{12}+s)}\right), \quad (4.14)$$

where we have used Eq. (4.12) and Eq. (4.13). Equation (4.8) then becomes

$$(\mathbf{r}_1|V|\mathbf{r}_1+\mathbf{x})=\frac{\pi}{x}\int_0^\infty r_{12}dr_{12}\int_{|r_{12}-2x|-r_{12}}^{2x}(r_{12}+s)ds(2l+1)\times(r_{12}|K_l|r_{12}+s)P_l\left(1-\frac{4x^2-s^2}{2r_{12}(r_{12}+s)}\right). \quad (4.15)$$

The variables $\mathbf{r}_2$, $\mathbf{r}_2'$, and the angle between these are, in terms of x and s,

$$|\mathbf{r}_2| = [r_1^2 + r_{12}^2 \mp 2r_1 r_{12}\cos\vartheta]^{\frac{1}{2}},$$
$$|\mathbf{r}_2'| = [(x \mp r_1)^2 + r_{12}^2 + 2r_{12}\cos\vartheta(x \mp r_1)]^{\frac{1}{2}}$$
$$\mathbf{r}_2\cdot\mathbf{r}_2' = r_1(r_1 \mp x) + r_{12}^2 + r_{12}\cos\vartheta(x \mp 2r_1),$$

with $\cos\vartheta$ given by Eq. (4.13).

In evaluating Eq. (4.15), we encountered considerable difficulty with the D-state contributions. The rapid variation of P_2 with s was difficult to represent accurately with the finest spacing of mesh points used in the calculation. We therefore replaced the $l=2$ part of the K matrix by a local approximation, i.e.,

$$(r_{12}|K_2|r_{12}+s) \rightarrow F(r_{12})\delta(s).$$

This is a very good approximation since for the range of K_2 for which the D state contributes appreciably, the K matrix is nearly local.

To complete the angular momentum reduction of the Hartree-Fock equation, the spherical harmonic expansion of $(\mathbf{r}_1|V|\mathbf{r}_1')$ is required [see Eq. (92) of BGW]. This is

$$(\mathbf{r}_1|V|\mathbf{r}_1') = \sum_l (2l+1)V_l(r_1,r_1')P_l(\hat{r}_1\cdot\hat{r}_1'), \quad (4.16)$$

or

$$V_l(r_1,r_1') = \frac{1}{2}\int_{-1}^{1} d\mu P_l(\mu)(\mathbf{r}_1|V|\mathbf{r}_1'), \quad (4.17)$$

with

$$\mu = \hat{r}_1\cdot\hat{r}_1'. \quad (4.18)$$

Since $(\mathbf{r}_1|V|\mathbf{r}_1')$ is given in Eq. (4.15) as a function of r_1 and x, it is convenient to make the transformation

$$\mu = \frac{r_1^2 + r_1'^2 - x^2}{2r_1r_1'}. \quad (4.19)$$

In these variables, we also have the relation

$$\mathbf{r}_1\cdot\mathbf{x} \equiv \mathbf{r}_1\cdot(\mathbf{r}_1' - \mathbf{r}_1) = \tfrac{1}{2}(r_1'^2 - r_1^2 - x^2). \quad (4.20)$$

Equation (4.17) then becomes, using Eq. (4.9),

$$V_l(r_1,r_1') = \frac{1}{2}\int_{|r_1-r_1'|}^{r_1+r_1'} \frac{x\,dx}{r_1r_1'} P_l\left(\frac{r_1^2 + r_1'^2 - x^2}{2r_1r_1'}\right) \times\left[V_0(r_1,x) + V_1(r_1,x)\frac{r_1'^2 - r_1^2 - x^2}{2r_1x}\right]. \quad (4.21)$$

To summarize the procedure used in determining the nonlocal potential V_{HF}, the following steps are required: (a) Starting from an initial set of eigenfunctions, determine $H(\mathbf{r}_2,\mathbf{r}_2')$ from Eq. (4.4); (b) for each value of $\mathbf{r}_1$ and $\mathbf{x} = \pm\mathbf{r}_1 x/r_1$, evaluate the s and r_{12} integrals in Eq. (4.15); (c) evaluate the x integral in Eq. (4.21) to determine the matrix elements $V_l(r_1,r_1')$. To this nonlocal potential must be added the local rearrangement potential V_R and the Coulomb potential. These are functions of the density and do not present any problem.

The second problem encountered in the numerical calculations is the solution of the eigenvalue equation [Eq. (3.7)] for the eigenvalues and eigenfunctions. This is complicated by the nonlocal potential which changes the usual Schrödinger equation into an integro-differential equation. A simple iterative method for solving such an equation is described by BGW. We again only give the required formulas.

The equation for the radial function R_{nlJ} of Eq. (4.2) is of the form

$$(E_i - H_0)\frac{R(r)}{r} = 4\pi\int r'dr'\, V(r,r')R(r'). \quad (4.22)$$

The BGW procedure is to evaluate the right-hand side of Eq. (4.22) using a solution resulting from a previous iterate or from an initial guessed input. The result is to replace Eq. (4.22) for the $(n+1)$st iterate by the differential equation

$$(E_i - H_0)\frac{R^{n+1}(r)}{r} = F^n(r)\frac{R^{n+1}(r)}{r} + \frac{G^n(r)}{r}\frac{dR^{n+1}(r)}{dr}. \quad (4.23)$$

The functions $F^n(r)$ and $G^n(r)$ are defined by the equations

$$F^n(r) = 4\pi r\int r'dr'\frac{V(r,r')}{D^n(r)} \times\left[R^n(r')R^n(r) + a^2\frac{dR^n(r')}{dr'}\frac{dR^n(r)}{dr}\right],$$
$$G^n(r) = 4\pi a^2 r\int r'dr'\frac{V(r,r')}{D^n(r)} \times\left[R^n(r')\frac{dR^n(r)}{dr} - R^n(r)\frac{dR^n(r')}{dr}\right] \quad (4.24)$$

with

$$D^n(r) = [R^n(r)]^2 + a^2\left[\frac{dR^n(r)}{dr}\right]^2. \quad (4.25)$$

The constant a was chosen in the numerical calculations to be 10^{-13} cm, which is the order of the range of the nonlocality of $V(r,r')$.

The form chosen for Eq. (4.23) and Eq. (4.24) is based on the two important features that the form is exact if the $(n+1)$st iterate is equal to the nth or if the range of the nonlocality in $V(r,r')$ is reduced to zero. A more detailed discussion of the derivation of Eq. (4.23) is given by BGW.

V. COMPUTATIONAL DETAILS

The program which performed the calculation on the IBM 704 consisted of two parts called HI and HII. HI takes a given set of radial wave functions $R_{nlj}(r)$ together with the K-matrix tables given in BGW for the attractive part [as well as the core contribution which itself depends on the local density and therefore on the $R_{nlj}(r)$] and carries out the integrations described previously to produce the $V_{lj}(r_1,r_1')$. HII takes the potentials $V_{lj}(r_1,r_1')$ and the wave functions R_{nlj}, generates the local equivalent-potentials $F_{nlj}(r_1)$, $G_{nlj}(r_1)$ [the Coulomb and rearrangement potentials being added into $F_{nlj}(r_1)$] and solves the BGW equation, [Eq. (4.23)] for a new set of wave functions $u_{nlj}(r_1)$.

The solutions of the modified Schrödinger equation [Eq. (4.23)] were obtained as follows. For a given trial energy, a Runga-Kutta scheme was used to integrate the wave function outward from the origin and inward from an external point (r_e) far outside the nucleus (10–12 fermis). The logarithmic derivatives were then compared at a point (r_0) which was outside the range of the nuclear forces (6–8 fermis). The initial conditions at r_e for the outer wave function were a small arbitrary value $R_{nlj}(r_e)$ and a logarithmic derivative equal to that which the appropriate Hankel function solution of the Schrödinger equation without Coulomb interaction would have. (Actually this refinement was not really necessary; a vanishing logarithmic derivative suffices.) The integration inward of the outer wave function was then carried out with the Coulomb interaction included. The comparison point r_0 was sufficiently far out so that the logarithmic derivative of the inner wave function was a very steep function of the trial energy in contrast to the logarithmic derivative of the outer wave function which is a slowly varying function of the trial energy. It is therefore necessary to have the trial energy search pattern converge quite accurately to the energy which matches the inner and outer logarithmic derivatives. After the energy eigenvalue has been found, the outer wave function is then renormalized to join smoothly to the inner wave function and then the entire wave function is normalized.

Since the initial wave functions were not those appropriate to the potentials V_{lj}, this process, which we call minor iteration, is repeated several times using the same V_{lj} until the F_{nlj}, G_{nlj}, R_{nlj} have converged to their proper values. In preliminary calculations in which the rearrangement energy was not included, the minor iterations converged quite well without any additional help. The rapid density dependence of the rearrangement energy caused the convergence to become much slower and sometimes to fail entirely. Therefore, the input and output wave functions in each minor iteration cycle were averaged and rapid convergence was obtained once again. The effect of the rearrangement energy on the convergence of the major cycles was not marked and no averaging was done between wave functions of consecutive major iterations.

After convergence of the minor iteration cycle, the R_{nlj} are then fed back into KI to produce a new set of nonlocal potentials V_{lj}. (This is called major iteration.) The whole procedure is started by introducing an essentially arbitrary local equivalent-potential $F_{nlj}(r_1) = V_{\text{init}}(r_1)$ (with $G_{nlj}=0$ usually) into HII and generating an initial set of wave functions R_{nlj}. The only requirement on $V_{\text{init}}(r_1)$ is that it accommodate the appropriate number of wave functions as bound states. The number of major iterations necessary to obtain convergence naturally depends on how close the initial set of wave functions is to a self-consistent set. It was found that even if this initial set was rather far away (say corresponding to a nuclear radius $1\frac{1}{2}$ times as large) not more than about 8 major iterations were necessary for self-consistency. On the other hand, if one had a self-consistent solution for one set of parameters and wished to vary one or more of these slightly (for instance vary the strength or slope of the core contribution to the K matrix), only two or three iterations were necessary.

The machine time required for these operations was as follows for the case of Zr^{90}, the largest nucleus studied. Each minor cycle took approximately 10 minutes, of which most of the time was used not in solving for the 21 wave functions but rather in a large amount of data shuffling on magnetic tapes due to lack of space in the fast memory of the machine (32 000 words in the 704). Most of the time was spent in the calculation of the V_{lj}(HI), the amount depending on the fineness of the meshes used in the integrations. Original hopes of being able to study many nuclei had to be abandoned when it was found that the meshes had to be considerably finer than those used in some of the earlier calculations. With the mesh finally settled upon, the time required for a single major iteration in the case of Zr^{90} became $4\frac{1}{2}$ hours.

TABLE II. Variation of calculated quantities in O^{16} with iteration of major and minor Hartree-Fock cycles.

Major iteration	Minor iteration	Neutron energy in $1s_{\frac{1}{2}}$ state	Proton energy in $1p_{\frac{1}{2}}$ state	Binding energy per particle	Rms radius (fermis)
I	1	−38.18	−6.69	−2.18	2.51
	2	−37.74	−6.75	−2.24	2.52
	3	−37.72	−6.80	−2.24	2.52
	4	−37.74	−6.82	−2.24	2.52
II	1	−37.03	−6.30	−2.08	2.55
	2	−37.19	−6.41	−2.07	2.55
	3	−37.22	−6.44	−2.07	2.55
III	1	−36.87	−6.36	−2.03	2.56
	2	−36.96	−6.40	−2.02	2.56
	3	−36.97	−6.41	−2.02	2.56
	4	−36.97	−6.42	−2.02	2.56
	5	−36.97	−6.42	−2.02	2.56

As an indication of the rate of convergence of the minor and major iteration cycles, we give in Table II for O^{16} the variation of two of the energy eigenvalues, of the total energy, and of the rms radius through several minor and major cycles. The convergence is clearly very rapid.

A large amount of experimentation was necessary in order to find a mesh which was both accurate and kept the time within reason. The necessity for a fine mesh is due to the detailed structure of the K matrix and the rapid dependence on the angle between r_{12} and r_{12}' in the relative D-state contribution. The final choice of mesh was set by the structure of the K-matrix tables and by the requirement that the results be unaffected by the coarseness of the mesh. The values taken were as follows (in fermis):

s mesh	17 points	$-0.60(0.05)0.20$
r_{12} mesh	13 points	$0.4(0.1)1.0(0.3)1.6(0.5)3.6$
x mesh	43 points	$0.0(0.5)2.1$
r_1' mesh	161 points	$-2.0(0.025)2.0$

r_1 mesh up to 40 depending on nucleus, interval (0.2).

VI. RESULTS

Before discussing the results, we shall describe some of the difficulties encountered in the calculations. The first problem was that we found it impossible to obtain values for the total energy which agreed with observed values. To see if this was due to a possible error in the K matrix obtained by BGW by transformation of the operator determined in the study of nuclear matter, the BGW procedure was inverted and the energy of nuclear matter redetermined. This involved evaluating the single-particle potential energy using Eq. (3.8) with plane waves for the single-particle eigenstates, and then taking appropriate matrix elements of $(r|V|r')$. The results for the potential energy agreed within a few percent with those obtained by Brueckner and Gammel[1] and also gave the correct binding energy for nuclear matter at a density corresponding to $r_0=1.02\times10^{-13}$ cm. Additional checks also verified both the strength of the repulsive core contribution and its density variation. Consequently, the incorrect values obtained for the energy of the finite nucleus could not be attributed to an incorrect K matrix. It is instead probable that the basic approximation made by BGW, that the correlation structure of the wave function is unaffected by density gradients (see Sec. III), is quantitatively in error. This affects most strongly the repulsive core contribution, apparently overestimating the many-body enhancement of the core energy. We have, therefore, slightly adjusted the parameter determining the core contribution, a decrease in strength of 10 to 20% being necessary to increase the binding energies to more reasonable values. (The actual changes made will be given below in discussing the numerical results.) We shall not attempt to give here any further justification for this change.

We also found it essential to include the rearrangement potential V_R of Eq. (3.12) in the single-particle potential. The effect appears first through a considerable shift in the single-particle energy, the inclusion of V_R being necessary to bring the energy eigenvalue of the last particle into approximate agreement with the separation energy. Another effect, which was not expected before the calculations were carried out, was that the nuclear density became much too high when the rearrangement potential was omitted. It was found that in the absence of this term, the nuclear density failed to stabilize near the density for which the energy of nuclear matter was a minimum, corresponding to $r_0=1.02\times10^{-13}$ cm.

This can be easily understood since the single-particle potential energy, if the rearrangement potential is absent, is too large and the wave functions are pulled toward the origin. This effect, which occurs only in the finite nucleus where the form of the wave functions must be determined, offsets the tendency of the system to adjust itself to minimize the energy. Another way of stating this result is that the Hartree-Fock self-consistency requirement in the wave functions and potentials is not necessarily the same as the requirement of minimum total energy in the sense of the nuclear matter calculation. Consequently, the rearrangement potential has a large effect on the results although the effect is only through the change of the wave functions, the energy still being given by the K-matrix expression of Eq. (2.1).

A. Energy Eigenvalues and Binding Energy

We first give the results for the energies of O^{16}, Ca^{40}, and Zr^{90} in Table III. The modification of the repulsive core contribution is indicated for each case. We also include the expectation value of the potential energy, including the rearrangement energy and Coulomb energy for each case. These tables show that even with the adjusted core strength the magnitudes of binding energies and separation energies are too small.[10] It is interesting to note, however, that the calculated differences between separation energies show better agreement with experiment. This is shown in Table IV. This agreement shows that the Coulomb and symmetry energies have reasonable values.

The spin-orbit splitting we find is due almost entirely to the odd-state spin-orbit force in the Gammel-Thaler potential. As was shown by BGW, this gives a single-particle spin-orbit potential which is not of Thomas form, although the potential does reduce to this form if the range of the two-body L-S potential is assumed to be very small. Figure 3 shows that the actual L-S potentials do not appear to be limited to regions of density gradient so that a Thomas form is incorrect.

[10] A. H. Wapstra, Physica 21, 367 and 385 (1955).

TABLE III. Calculated and experimental energies for O^{16}, Ca^{40}, and Zr^{90}. The core strength has been reduced to 0.825 of the normal value for O^{16}, and to 0.90 of the normal value for Ca^{40} and Zr^{90}. The energies are in Mev.

Element	State	Potential energy Neutron	Potential energy Proton	Eigenvalue Neutron	Eigenvalue Proton	Experimental separation energy Neutron	Experimental separation energy Proton	Total energy per particle Calc.	Total energy per particle Expt.
O^{16}	$1s_{1/2}$	−58.0	−53.0	−44.3	−39.6				
	$1p_{3/2}$	−40.1	−35.2	−19.0	−14.6			−4.41	−7.98
	$1p_{1/2}$	−34.4	−29.7	−14.9	−10.7	−15.60	−12.11		
Ca^{40}	$1s_{1/2}$	−82.4	−72.1	−70.1	−60.0				
	$1p_{3/2}$	−65.2	−55.1	−44.7	−35.1				
	$1p_{1/2}$	−59.2	−49.3	−38.6	−29.2			−6.12	−8.55
	$1d_{5/2}$	−48.3	−38.2	−20.6	−11.6				
	$2s_{1/2}$	−40.5	−30.0	−16.0	−7.3				
	$1d_{3/2}$	−39.6	−29.6	−13.4	−4.9	−15.98	−8.34		
Zr^{90}	$1s_{1/2}$	−87.7	−72.0	−79.5	−64.0				
	$1p_{3/2}$	−77.8	−62.3	−62.8	−47.7				
	$1p_{1/2}$	−75.5	−60.2	−59.8	−44.9				
	$1d_{5/2}$	−66.6	−51.4	−44.5	−29.9				
	$2s_{1/2}$	−62.2	−46.5	−38.6	−23.8			−5.80	−8.67
	$1d_{3/2}$	−63.7	−48.6	−40.2	−25.7				
	$1f_{7/2}$	−55.4	−40.2	−26.2	−12.0				
	$1f_{5/2}$	−51.2	−36.0	−20.5	−6.6				
	$2p_{1/2}$	−47.5	−31.0	−17.0	−3.2		−8.80		
	$1g_{9/2}$	−44.1		−8.5		−12.37			

The calculated L-S splittings are given in Table V. It is not easy to compare these directly with experiment although the order of magnitude is certainly correct. A more direct comparison with experiment can be made by using the separation energy in Zr^{90}. In this case the difference of 5.3 Mev between the last neutron in a $1g_{9/2}$ state and the last proton in a $2p_{1/2}$ state is largely a result of the shift of these levels due to the spin-orbit force. In the absence of this force, the $2p_{1/2}$ level would drop about 1.0 Mev and the $1g_{9/2}$ level would rise about 4.1 Mev, so that the separation energies would now be nearly the same, in disagreement with the observed difference of 3.57 Mev.

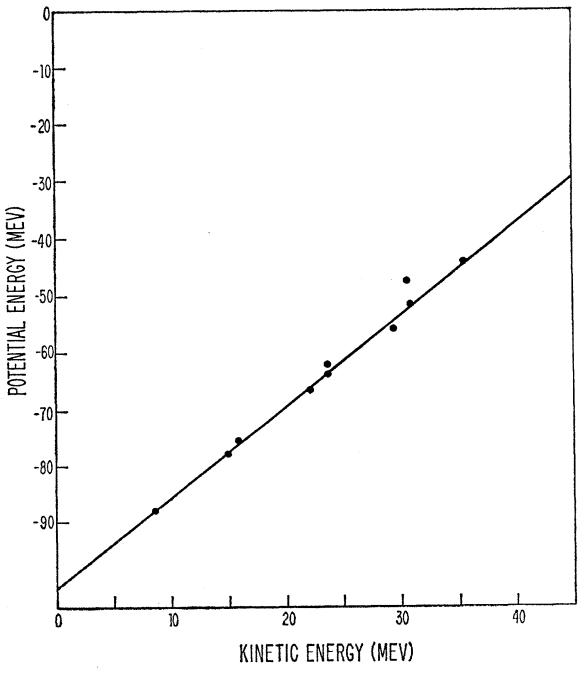

FIG. 1. Potential energy as a function of kinetic energy for the neutrons in Zr^{90}. The straight line corresponds to an effective mass of 0.39.

We have investigated in some detail the effects on the energy and mean radius of changes in the core repulsion. We changed not only the core strength but also the rate of variation of the core energy with density. The core contribution has a density dependence[2]

$$K_{\text{core}}=\text{constant}\frac{1-b/\bar{r}_0}{1-b/r_0}, \tag{6.1}$$

with

$$\tfrac{4}{3}\pi r_0^3=\rho^{-1}, \tag{6.2}$$

where ρ is the density, and $\bar{r}_0$ the mean spacing in

TABLE IV. Difference in separation energy for neutrons and protons. The energies are in Mev.

	Calculated	Experimental
O^{16}	4.2	3.49
Ca^{40}	8.5	7.64
Zr^{90}	5.3	3.57

TABLE V. Spin-orbit splitting in Mev.

	O^{16} Neutron	O^{16} Proton	Ca^{40} Neutron	Ca^{40} Proton	Zr^{90} Neutron	Zr^{90} Proton
$1p_{1/2}-1p_{3/2}$	4.1	3.9	6.1	5.9	3.0	2.8
$1d_{3/2}-1d_{5/2}$			7.2	6.7	4.3	4.2
$1f_{5/2}-1f_{7/2}$					5.7	5.4

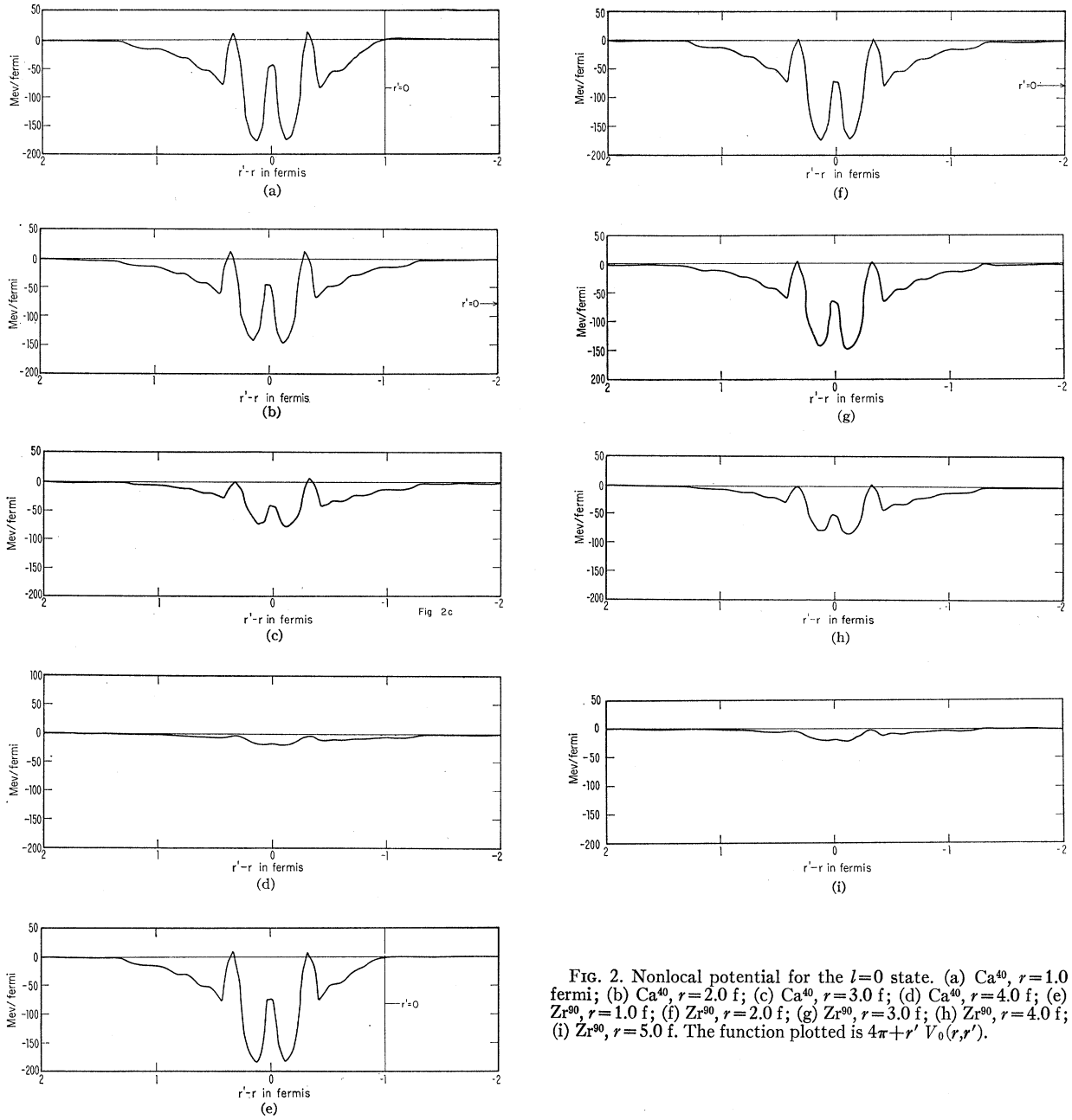

FIG. 2. Nonlocal potential for the $l=0$ state. (a) Ca^{40}, $r=1.0$ fermi; (b) Ca^{40}, $r=2.0$ f; (c) Ca^{40}, $r=3.0$ f; (d) Ca^{40}, $r=4.0$ f; (e) Zr^{90}, $r=1.0$ f; (f) Zr^{90}, $r=2.0$ f; (g) Zr^{90}, $r=3.0$ f; (h) Zr^{90}, $r=4.0$ f; (i) Zr^{90}, $r=5.0$ f. The function plotted is $4\pi+r' V_0(r,r')$.

nuclear matter, i.e., $\bar{r}_0=1.07\times10^{-13}$ cm. The density variation of K_{core} can therefore be changed by varying the parameter b in Eq. (6.1). We give in Table VI the mean binding energy and also the rms radius for several cases. These results show that the answer is only slightly changed by variations in the core density dependence, but that the mean energy and rms radius change quite appreciably with change in the core strength. The increase in binding energy as the core is weakened is accompanied by a decrease in rms radius, the greater attraction associated with larger binding energy pulling in the wave functions. This tendency

TABLE VI. Effects on mean energy and rms radius of changes in core strength, core density variation, and rearrangement energy.

	Core strength[a]	b[a]	E_{av}	R_{rms}
O^{16}	1.00	1.00	−2.02	2.56
	0.825	1.00	−4.41	2.40
Ca^{40}	1.00	1.00	−3.89	3.01
	0.90	1.00	−6.12	2.88
	1.00	1.30	−4.13	3.04

[a] Measured in units of normal values.

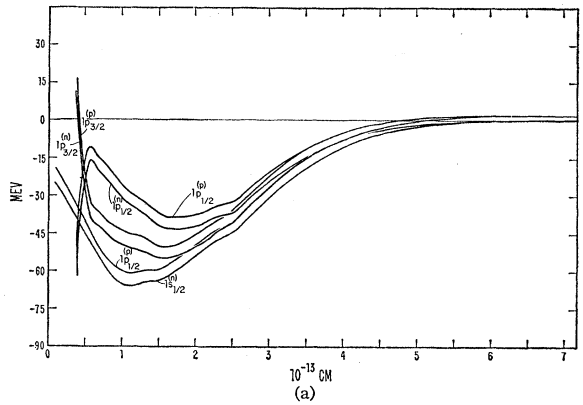
MEV
10^{-13} CM

(a)

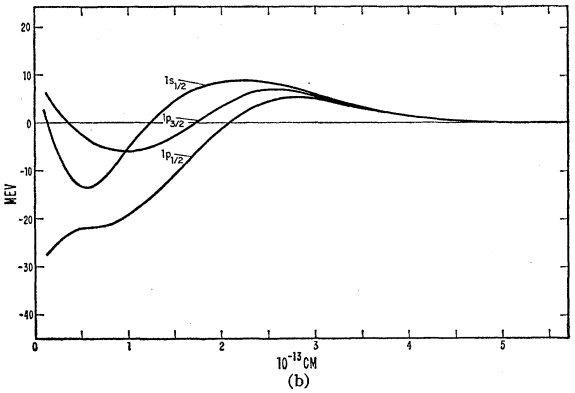
MEV
10^{-13} CM

(b)

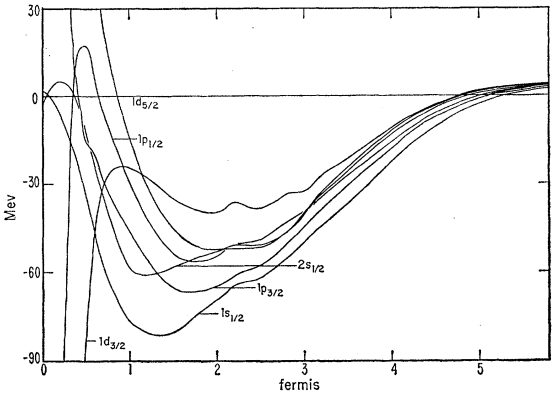
Mev
fermis

(c)

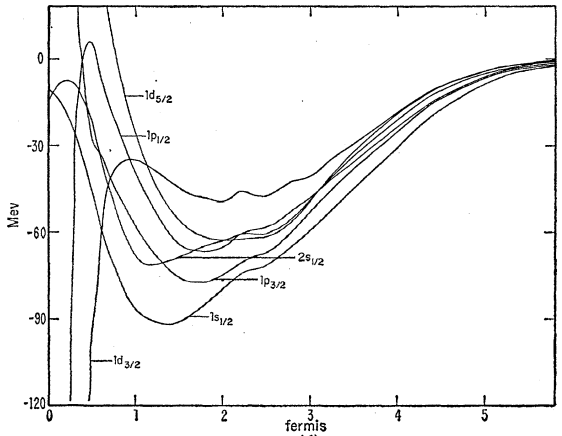
Mev
fermis

(d)

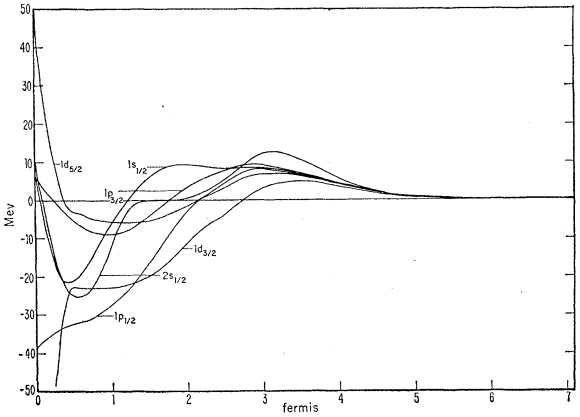
Mev
fermis

(e)

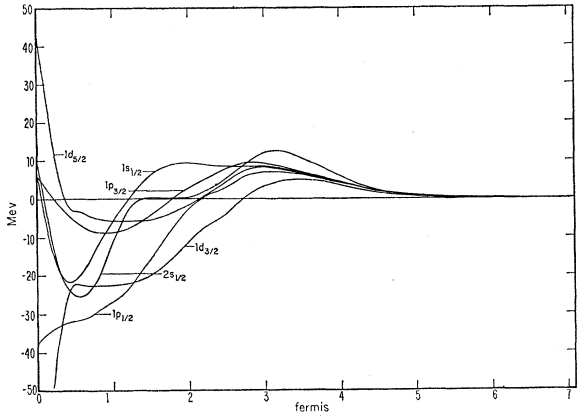
Mev
fermis

(f)

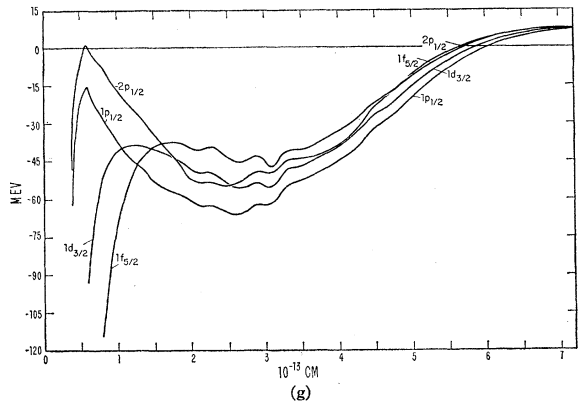
MEV
10^{-13} CM

(g)

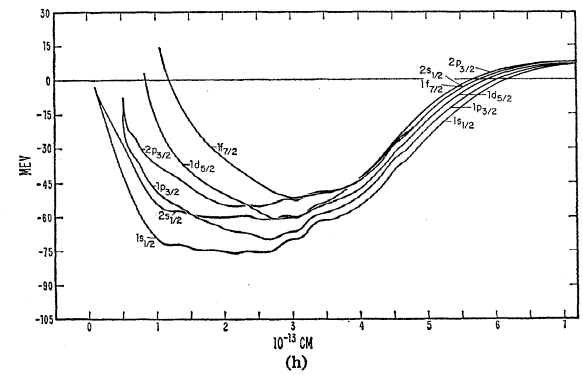
MEV
10^{-13} CM

(h)

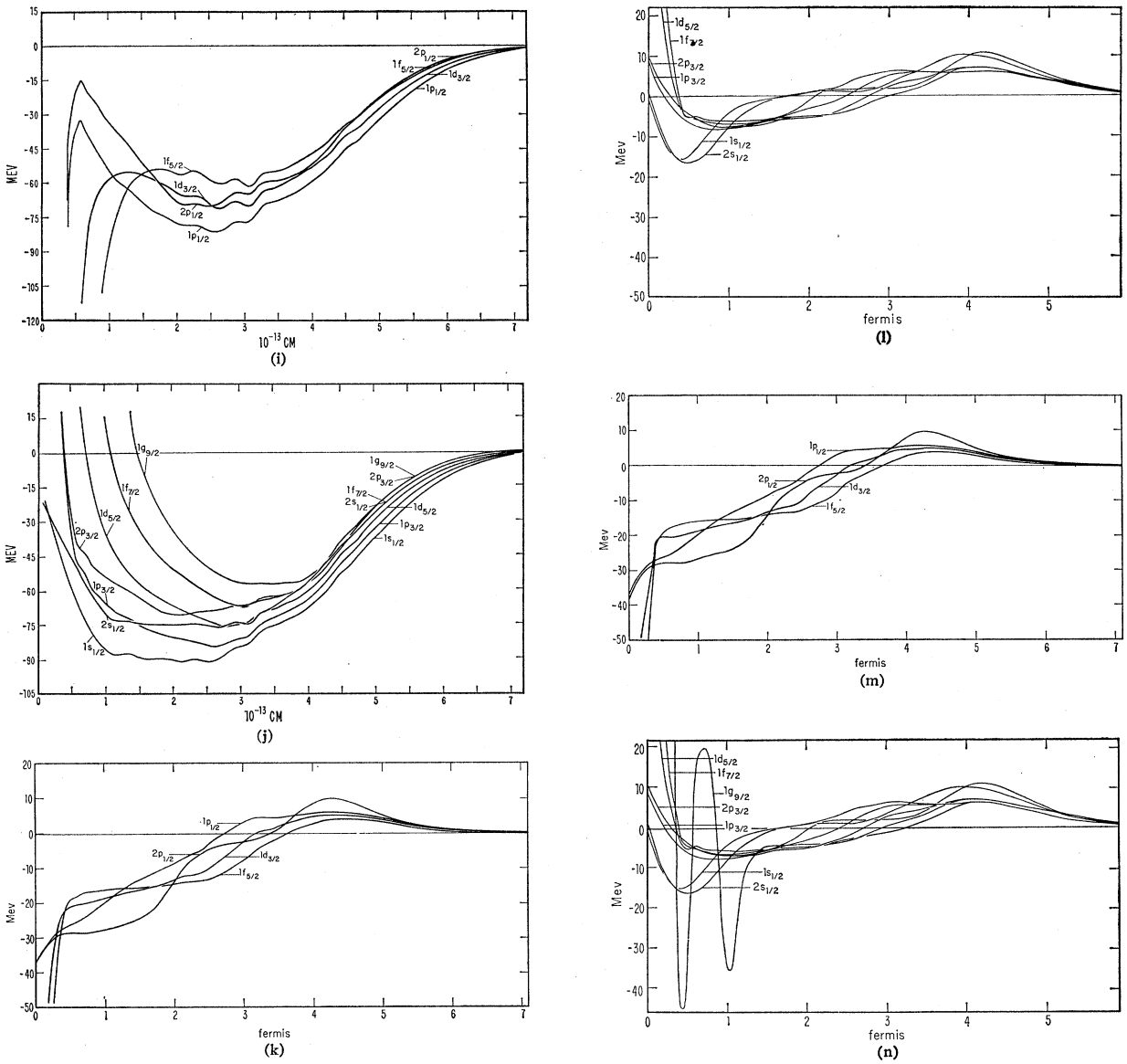

FIG. 3. The potential functions F and G defined in Eq. (4.24). (a) F for O^{16}; (b) G for O^{16}; (c) F for the protons in Ca^{40}; (d) F for the neutrons in Ca^{40}; (e) G for the protons in Ca^{40}; (f) G for the neutrons in Ca^{40}; (g) F for the protons with $j=l-\frac{1}{2}$ in Zr^{90}; (h) F for the protons with $j=l+\frac{1}{2}$ in Zr^{90}; (i) F for the neutrons with $j=l-\frac{1}{2}$ in Zr^{90}; (j) F for the neutrons with $j=l+\frac{1}{2}$ in Zr^{90}; (k) G for the protons with $j=l-\frac{1}{2}$ in Zr^{90}; (l) G for the protons with $j=l+\frac{1}{2}$ in Zr^{90}; (m) G for the neutrons with $j=l-\frac{1}{2}$ in Zr^{90}; (n) G for the neutrons with $j=l+\frac{1}{2}$ in Zr^{90}. The plotted functions are $rF(r)$ and $rG(r)$.

can be offset by an increase in the rearrangement energy which is repulsive and acts to prevent increase of the density. We have not, however, explored this possibility further.

Another interesting feature of the single-particle energies is the variation of the expectation value of the potential energy as the state is changed. In Fig. 1, we plot the potential energy including the rearrangement energy and eigenvalues against the kinetic energy for the neutrons in Zr^{90}. The straight line which gives an approximate fit to the computed values corresponds to an effective mass of $m^*/m=0.39$ which is much less than the value of about 0.65 found in nuclear matter.[2] This difference is an effect of the finite nucleus and of the greater extension of the wave functions of the more weakly bound nucleons.

Before we end our discussion of the energy, we wish to re-emphasize the quite indirect connection between the energy eigenvalues and the total energy. Not only half of the potential energy but also the rearrangement energy must be subtracted in going from the eigenvalues to the total energy. This is apparent from a comparison of Eq. (3.4) for the total energy with Eq. (3.7) for the single-particle eigenvalue.

B. Single-Particle Potentials and Wave Functions

We now turn to a discussion of the structure of the nonlocal potential in which a particle moves. We choose the same K-matrix parameters as in Table III. The nonlocal potential is most easily given in terms of the angular momentum decomposition of Eq. (4.16). Except for the effect of the spin-orbit force, the successive terms $V_l(r,r')$ depend only weakly on l since the distance over which the spherical harmonics vary rapidly as in general large compared to the range of the nonlocality in $V(\mathbf{r},\mathbf{r}')$. If for example, $V(\mathbf{r},\mathbf{r}')$ is a local potential, then $V_l(r,r')$ is independent of l. Thus we content ourselves with giving on the case $l=0$.

To express the form of the nonlocal potential most simply, we give $V_0(r,r')$ in Fig. 2 for Ca^{40} and Zr^{90} for several values of r. The values of r are chosen to give representative points in the density variation, including central and surface points for which the potential has quite different structure.

The nonlocality in $V_l(r,r')$ is due to two quite different effects. First, even for a local two-body potential, the effects of exchange can be most easily represented in the Hartree-Fock equations as a nonlocality. This is evident from Eq. (3.8) since even for a local interaction, the single-particle potential is nonlocal. This effect has a range of the order of the full range of the two-body interaction. Added to this effect is that due to the nonlocality in the K matrix. This is due to the great strength of the two-body interaction which strongly polarizes the wave function at small distances, this appearing in the K matrix as a nonlocality. The range of this effect is less than 10^{-13} cm and in this region contributes more strongly to the nonlocality of $V_l(r,r')$ than the exchange effect.

The nonlocal character of the single-particle potential also can be exhibited in a way analogous to the "effective mass" concept of nuclear matter,[2] where it is known that the nonlocality manifests itself through the velocity dependence of the single-particle potential energy. In the finite nucleus, this is most easily exhibited by making a local replacement of the nonlocal single-particle potential. We first give in Fig. 3(a) through (m) the functions F and G which appear in Eq. (4.23). The equivalent potential F plays the same role in the Schrödinger equation as the usual shell-model potential with which it is most directly compared. It is apparent from these figures that both F and G change considerably as either J or n the principal quantum number, is changed.

TABLE VII. Root-mean-square radii in fermis.

Nucleus	Neutron	Proton	Total	Experiment
O^{16}	2.38	2.41	2.40	2.57
Ca^{40}	2.84	2.91	2.88	3.49
Zr^{90}	3.64	3.56	3.60	4.24

The radial functions determined by solution of the eigenvalue problem are given in Fig. 4. These differ from conventional wave functions largely as a result of the state dependence of the potential. The inner-shell wave functions are pulled in more strongly than for a conventional shell model and also fall off more rapidly near the nuclear surface since the eigenvalues are much lower than for a static potential.

C. Density

In Table VII we give the rms radii for neutrons, protons, and for the total density, together with the values deduced from experiment.[11] The computed values are too small by 6% in O^{16} and 20% in Ca^{40} and Zr^{90}. It was found to be very difficult to eliminate this error by any simple changes in the K matrix, considerable variations in core structure and in rearrangement energy having only slight effect on the mean radius. This difficulty is particularly marked when it is realized that our binding energies were also too small, and that attempts to increase the binding led to further decrease in radius. It is likely that this problem can be partially attributed to the short range of the Gammel-Thaler two-body potentials and possibly to our treatment of the correlation structure in the surface.

We give the densities as a function of the radius in Figs. 5(a), (b), (c). These results together with the rms radii show that there is very little separation between the neutron and proton densities, the rms proton radius exceeding the rms neutron radius by 0.03 fermi in O^{16} and 0.07 fermi in Ca^{40} due to the Coulomb repulsion. In Zr^{90} the reverse is true, the neutron radius being the larger by 0.08 fermi. These differences are very small, the neutron and proton densities being kept together by the effects of the symmetry energy. This result agrees with experimental measurements of the neutron and proton distribution.[12]

From Fig. 5 we can determine the surface depth, i.e., the distance over which the density falls off from 90% to 10% of the central value. This is 1.7 fermis in O^{16}, 2.8 fermis in Ca^{40}, and 2.2 fermis in Zr^{90}. These are to be compared with the value of (2.4 ± 0.2) fermis deduced from experiment.[11]

One other comparison of interest is between the density and the potential. We give this in Fig. 6 for Ca^{40} and Zr^{90}, taking the total density and the equivalent potential $F(r)$ defined by Eq. (4.24) for the highest neutron state, $1d_{5/2}$ for Ca^{40} and $1g_{9/2}$ for Zr^{90}. In both cases the potential radius is about 0.75 fermi greater than the density radius. This difference is largely due to two effects previously discussed,[13] which are: (a)

[11] D. G. Ravenhall, Revs. Modern Phys. **30**, 414 (1958).
[12] A. Abashian, R. Cool, and J. W. Cronin, Phys. Rev. **104**, 855 (1956).
[13] K. A. Brueckner, Revs. Modern Phys. **30**, 561 (1958).

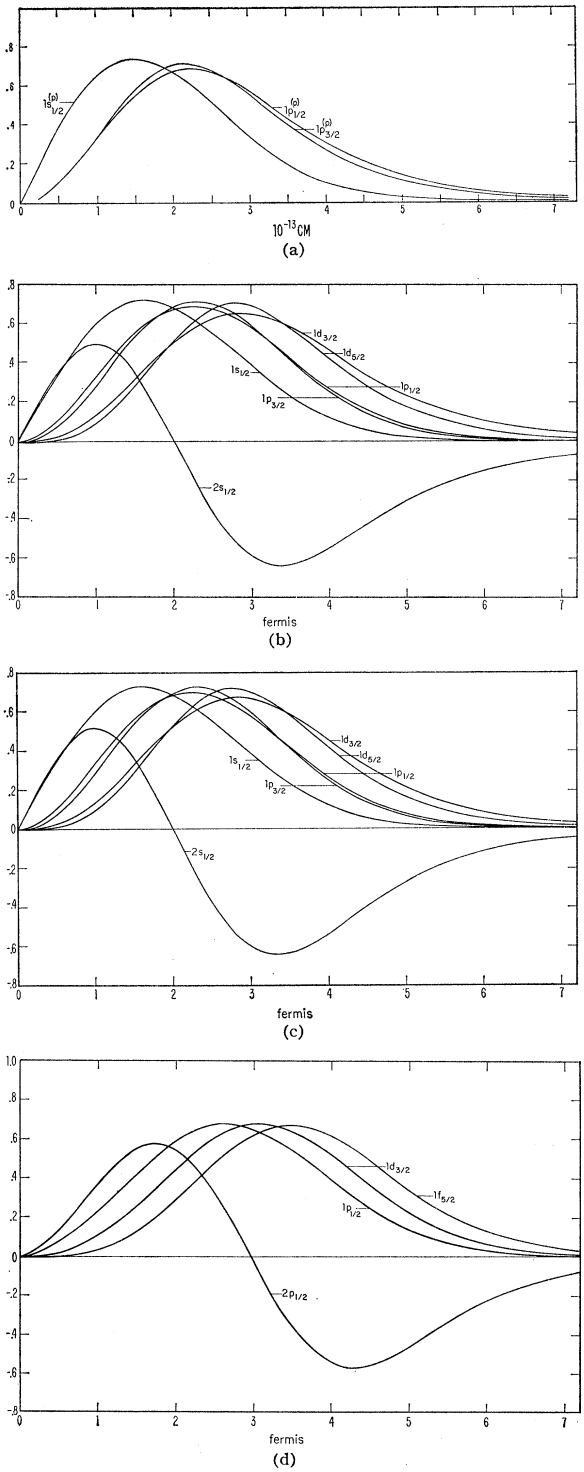

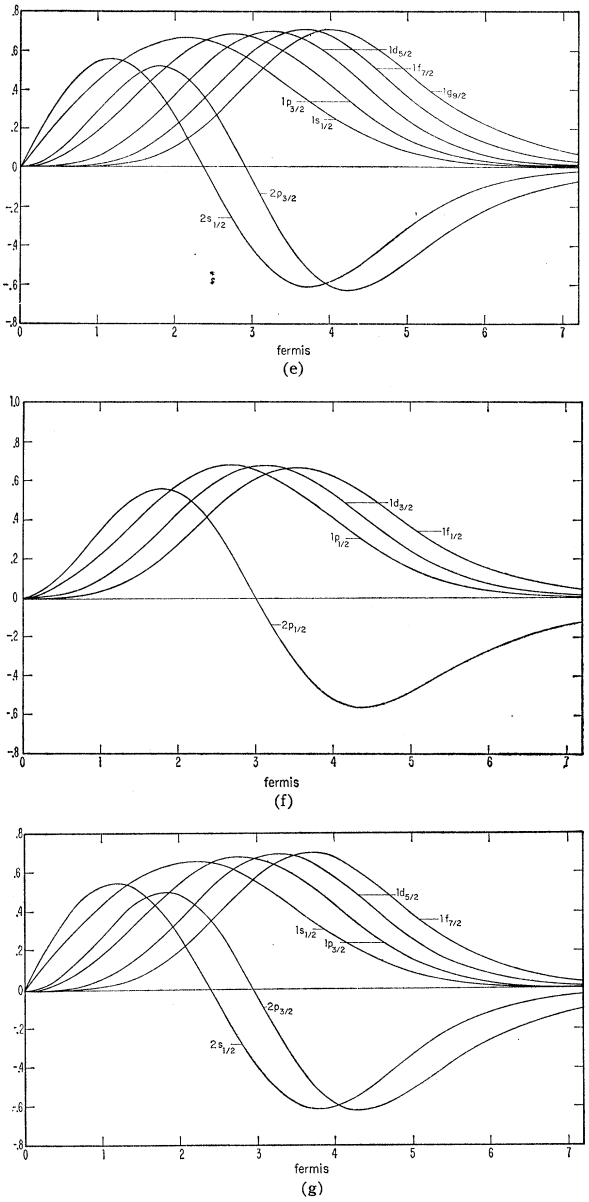

FIG. 4. The radial wave functions (a) for the neutrons and protons in O^{16}; (b) for the protons in Ca^{40}; (c) for the neutrons in Ca^{40}; (d) for the protons with $j=l-\frac{1}{2}$ in Zr^{90}; (e) for the protons with $j=l+\frac{1}{2}$ in Zr^{90}; (f) for the neutrons with $j=l-\frac{1}{2}$ in Zr^{90}; (g) for the neutrons with $j=l+\frac{1}{2}$ in Zr^{90}.

finite range of interaction; (b) nonlinear variation of potential energy with density. The computed separation between density and potential is about equal to that observed experimentally.[14]

[14] S. Fernbach, Revs. Modern Phys. **30**, 414 (1958).

VII. DISCUSSION

The results of this paper show that the BGW theory of finite nuclei, based on the K-matrix theory of nuclear matter, does not give fully quantitative results for the properties of the nuclei studied, O^{16}, Ca^{40}, Zr^{90}.

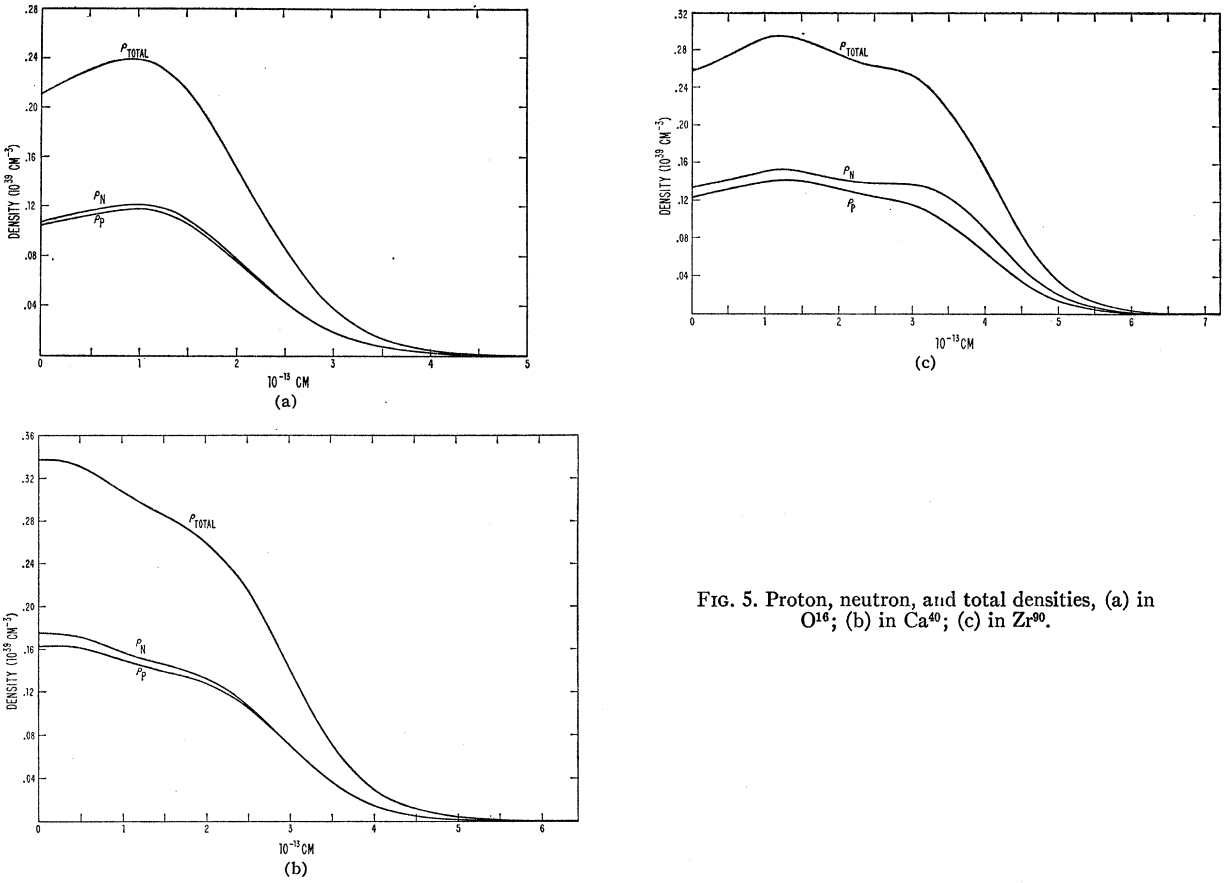

FIG. 5. Proton, neutron, and total densities, (a) in O^{16}; (b) in Ca^{40}; (c) in Zr^{90}.

Since this theory already has given accurate results for nuclear matter, it is clear that the finite systems prevent problems not fully taken into account by the BGW theory. We have already suggested that the difficulty may lie in the approximation which treats the nuclear correlation as independent of the density gradient. The rearrangement energy also has a fundamental role in the finite nucleus in contrast to nuclear matter, and our treatment of the rearrangement effects may not be sufficiently quantitative.

The difficulties of our calculations lie mainly in our inability to obtain sufficient binding energy and large enough radii. It should be emphasized, however, that the error we find in binding energy is the result of about an 8% error in potential energy so that the discrepancy is in this sense small. The problem with the radii is, however, more interesting in that attempts to decrease the radius tend to lead further decreases in binding energy. The only obvious solutions to this problem lie in the direction of increase in the range of the two-body interaction or of increase in the repulsive effects of the rearrangement energy. The former change seems inacceptable since the range of the interaction is determined by two-body scattering data; the latter change may be correct but was not justified by the results obtained from the K-matrix studies of nuclear matter. We therefore must regard this question as unresolved by our studies.

Our results, aside from the quantitative questions of binding energy and radius, do give insight into many other nuclear properties. The level sequence we find, which is largely fixed by the spin-orbit interaction, is in good agreement with experiment. This is also true of the relationships among our calculated separation energies for neutrons and protons and the mean binding energy. This agreement also shows that our nuclei are properly beta-stable so that we correctly follow the line of nuclear stability.

The general features of the single-particle potential which we have determined are also new and of interest. The marked nonlocality of the potential manifests itself clearly in the strong state dependence of the equivalent potential. The nonlocality also is evident in the wave functions which have appreciable curvature at their nodes, this being possible only because of the finite nonlocal range. We also find a difference of about 0.75 fermi between the potential and density radius, this explaining a feature deduced from experiment which was not before theoretically understood.

The details of the density distribution are also new

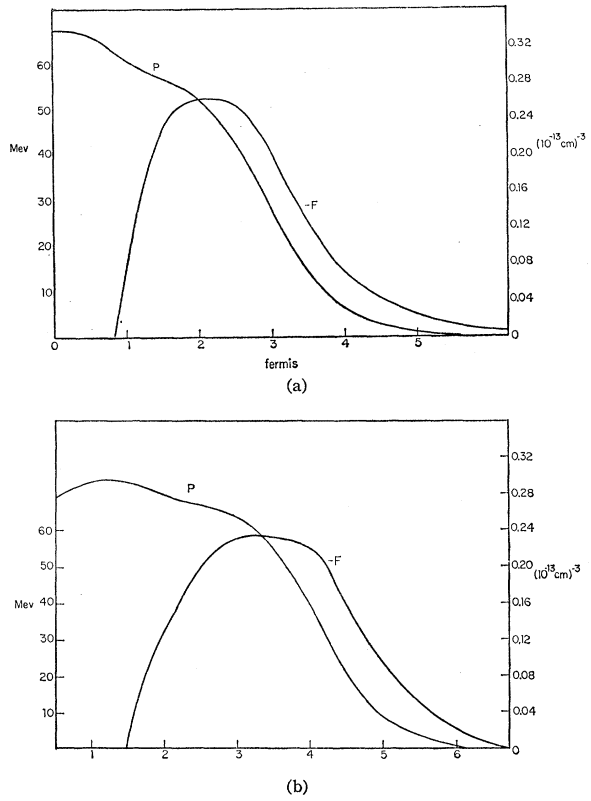

FIG. 6. (a) $F(r)$ for the highest neutron state in Ca^{40} and the total density as a function of radius. (b) $F(r)$ for the highest neutron state in Zr^{90} and the total density as a function of radius.

and interesting. They are characterized by the tendency of neutrons and protons to maintain a uniform density ratio so that there is very little separation in mean radii. We also find density surface thicknesses which agree well with experiment. The surface density is fixed partially by the finite force range, but also by the strong state dependence of the single-particle potentials. This effect increases the rate of fall off of the inner shell wave functions near the surface and so decreases the surface depth.

In conclusion we summarize the applications which have been made of the many-body theory to nuclear matter and finite nuclei. These are:

Nuclear matter:
- volume energy
- symmetry energy
- density
- compressibility
- effective mass
- optical potential.

Finite nuclei:
- binding energy
- spin-orbit splitting
- separation energy
- density distribution
- neutron-proton density relation
- surface depth
- potential-density relations
- state dependence of single potential
- nonlocality of single-particle potential.

The theory gives quantitative predictions for nuclear matter and semiquantitative predictions for finite nuclei.

ACKNOWLEDGMENT

We are indebted to Dr. John L. Gammel for many discussions of the problems of this work.